Eur**opean** J**ournal of** Chem**istry**

Uptake of selected heavy metals from contaminated waters utilizing cost-effective and environmentally friendly biosorbents prepared from the residues of a traditionally fermented Ethiopian alcoholic beverage (*Tella*)

Tesfahun Kebede [1], Henok Getachew [1], Abi Legesse [2], and Negussie Megersa [2,*]

[1] *Department of Chemistry, College of Natural and Computational Sciences, Haramaya University, PO Box 138, Haramaya, Ethiopia*
[2] *Department of Chemistry, College of Natural and Computational Sciences, Addis Ababa University, PO Box 1176, Addis Ababa, Ethiopia*

* *Corresponding author at: Department of Chemistry, College of Natural and Computational Sciences, Addis Ababa University, PO Box 1176, Addis Ababa, Ethiopia.*
 e-mail: negussie.megersa@aau.edu.et *(N. Megersa).*
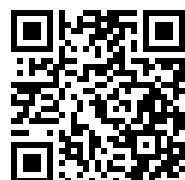
RESEARCH ARTICLE

ABSTRACT

In the current study, the adsorption capacity of *Tella* residues (residues of fermented alcoholic beverage) for quantitative uptake of Cu(II), Cd(II), Zn(II) and Pb(II) was evaluated. Chemical treatment of the local beer residue (LBR) has improved the removal efficiency of the adsorbent, which was achieved at pH = 5, 1.0 g adsorbent, 50 mg/L initial concentration, 180 min contact time and agitation speed of 100 rpm. The adsorption was found to fit the Langmuir adsorption isotherm model, and the theoretical equilibrium capacities were well fitted with the experimental equilibrium capacities, resulting in chemical adsorption (chemisorptions) on the adsorbent surface while the equilibrium kinetics follows the pseudo-second-order. The adsorption capacity (Q_o) of LBR decreases in the following order: Zn(II) > Cu(II) > Pb(II) > Cd(II) as metal concentration ranged from 20-200 mg/L. Thermodynamic parameters, including standard free energy ($\Delta G°$), enthalpy ($\Delta H°$) and entropy ($\Delta S°$) were calculated to predict the nature of adsorption. The negative values of $\Delta G°$ and the positive value of $\Delta H°$ indicate that the adsorption process was spontaneous and endothermic. Adsorption capacities were found to increase when the temperature ranged from 25-60 °C. Thus, the findings suggest a promising application of LBR as an alternative low-cost novel adsorbent for the removal of toxic heavy metals from wastewater.

1. Introduction

Heavy metals are chemical substances that have a specific gravity greater than 5 g/cm³ and atomic weights ranging from 63.5 to 200.6 g/mol [1,2]. The most commonly known heavy metal ions include Cu(II), Zn(II), Ni(II), Pb(II), Cd(II), and Hg(II) ions, among which, Cd(II), Pb(II), Hg(II), and As(III) have been identified as the most dangerous heavy metal ions according to the report by the World Health Organization (WHO) [3]. One of the common characteristics of heavy metals is their chronic toxicity. They are also known to cause environmental threats to living organisms and habitats due to their non-biodegradability, bioaccumulation, environmental stability, biotoxicity, and persistence characteristics. Moreover, they are considered subtle and silent killers, which have the great power to affect human life at any time [4,5]. The primary causes of heavy metal ion pollution are untreated industrial discharges, including those from coal-firing power plants, mining, alumina refineries, metallurgical industries, heavy chemicals, chlor-alkali indust-ries, battery industries, dyes and pigments, fertilizers, metal smelters, paints and ceramics, tanneries, textiles and other similar sources. Additionally, an astonishing 80% of waste-

water worldwide is discharged into the environment without undergoing treatment. This risk is most acute in developing countries, where a staggering 90% of wastewater is released into the environment without proper treatment [6]. In recent years, the accelerating pace of global industrialization has also resulted in an excessive discharge of harmful metals into the environment, which pose significant threats to human health and the ecosystem.

These days, public awareness on the deleterious impact of chemical contaminants from various compartments of water bodies (*i.e.*, groundwater, rivers, and lakes, *etc.*), are rapidly growing, as the overall effect observed on all living things such as humans, animals, plants, and others, since they all consume water in one way or the other. The water contaminated by heavy metals can also easily contaminate the soil, which in turn contaminates the plants [7,8]. In order to effectively mitigate and, whenever feasible, eliminate the potential harm caused by toxic metals, it is essential to consistently pinpoint probable sources and take appropriate measures to minimize or eradicate uncontrolled releases. To achieve reliable solutions, it requires prior technical planning and development of strategic thoughts, which should be sought for the removal of these

metals from effluents containing heavy metals before polluting environmental waters [9,10].

In recent years, different countries have made significant progress in reducing the discharge of harmful metals into the environment. This has been achieved through stricter regulations, enhanced cleaning technologies, and changes in industrial practices. Despite these advances, there is still a need for economical and environmentally friendly strategies to remove toxic metals. Different analytical techniques have been developed and applied for the quantitative removal of these metal ions from wastewater samples, and commonly used methods include chemical precipitation [11-13], ion exchange [14,15], membrane technology [16-18], activated carbon adsorption [19-22], *etc*. All the methods indicated have their own intrinsic advantages and disadvantages. Chemical precipitation is inefficient, especially when the concentration of the metal ion is below 50 mg/L in the aqueous solution. Furthermore, such treatments are known to produce enormous amounts of sludge and generate secondary waste that need further treatment/purification, which requires high capital and operating costs [23]. Other methods, such as membrane technology, ion exchange, and activated carbon adsorption, are more expensive. Therefore, a newer and more cost-effective method with an efficient capacity to remove toxic metals from polluted waters should be adapted. Therefore, the utilization of biosorbents seems to be a preferable option due to the fact that the demerits described in the methods mentioned above could be greatly reduced [24,25].

Biosorption is an adsorption technique that uses low-cost biomass to sequester toxic heavy metals and is specifically advantageous for the removal of toxicants from industrial effluents. The need for a cost-effective and readily available adsorbent has led to the choice of materials derived from agricultural and biological sources, as well as industrial waste products, as adsorbents to significantly reduce the levels of harmful heavy metals in the environment to acceptable limits at an economical cost. Agricultural waste, including wheat bran [26,27], walnut, hazelnut and almond shell [28,29], rice husk [30,31], rice straw [32], barley hull [33], sugarcane bagasse [1], sawdust of wood and wheat straw [34,35], and *Teff* straw [36] have been utilized as efficient sorbents for the removal of heavy metals from polluted aqueous samples.

In this study, disposable residues that were settled during the *'Tella'* fermentation process were utilized as a cost-effective biosorbent for the quantitative uptake of metal ions from contaminated water samples. *Tella* is a traditionally fermented home-brewed local alcoholic beverage commonly consumed in all region of the country, Ethiopia [37]. It is fermented from different vernacular grains and is a malt of substrates like barley, wheat, maize, millet, sorghum, *Teff* and several other cereals [37,38].

The preparation and fermentation of the "*Tella*" drink follows a series of steps described in published literature [37-40]. In the context of its application for this study, at the end of fermentation, most of the materials that settle at the bottom of the container, mainly the clay pot, are obtained after about 12 days. The residue settled at the bottom, locally called '*Atela*', was used as a biosorbent, named in this study as Local Beer Residue (LBR) for the uptake of metal ions [40]. The filtrate or supernatant, separated from the residue, is normally served to consumers.

To date, there has been no literature report on the removal of heavy metal ions by LBR residues from contaminated water samples. Hence, in the current study, it is intended to explore the adsorption capacity of this residue towards the selected metal ions removal; namely, Pb(II), Cd(II), Zn(II) and Cu(II) from contaminated aqueous samples.

2. Experimental

2.1. Experimental site and equipment

The fermented alcoholic beverage commonly named *'Tella'* is the generic name for 'Ethiopian Local Beer'. It was prepared and collected from a vendor house in Dire Dawa city; located at 9°36'N latitude and 41°52'E longitude, and an elevation above sea level of 1180 m. It is one of the administrative regions located in eastern Ethiopia, close to Haramaya University (HU). The preparation of *Tella* residues, *i.e.*, local beer residue (LBR) as potential novel adsorbents, and the batch sorption experiments were performed at the postgraduate research laboratory of the Department of Chemistry of the HU. The determination of target metal ions concentration was conducted at the HU Soil Science Laboratory using Flame Atomic Absorption Spectroscopy, FAAS (Model210/211 VGP). Functional group identification before and after absorption was achieved with the FT-IR spectrometric instrument (Shimadzu, 1730, Japan) and was carried out at the Analytical Instrumentation Laboratory of the Department of Chemistry of Addis Ababa University (AAU). The pH of the sample solution was manually adjusted by the pH meter (MP 220), mainly for the pH of the working solutions, which was achieved using 0.10 M NaOH and 0.10 M HCl solutions. A rotary shaker (Orbital Shaker SO1, UK), was used to shake the solutions. Ultrapure water was obtained by purifying with a 8000 Aquatron water Still double distiller (Bibby Scientific, Staffordshire, UK) and a deionizer (EASY Pure LF, Dubuque). In this study, a 1.5 mm sieve and a hot air oven (Contherm 260 M) were also used.

2.2. Chemicals and reagents

The analyte standards used were of analytical reagent grade chemicals including $Cd(NO_3)_2 \cdot 4H_2O$, $Cu(NO_3)_2 \cdot 4H_2O$, $Pb(NO_3)_2$, and $Zn(NO_3)_2$. All inorganic salts were dissolved in deionized water to prepare the corresponding adsorbates, *i.e.* metal-ion solutions. Other common chemical substances such as H_2SO_4 (98%, laboratory reagent, LOBA, India), HNO_3 (69%, LR, Breckland Scientific Supplies, UK), sodium hydroxide and hydrochloric acid, both obtained from Sigma-Aldrich (St. Louis, Mo, USA), were used in this study. The pH meter was standardized using buffer solutions; with pH values of 4, 7, and 9.

2.3. Preparation and modification of LBR

The collected adsorbent of local beer residue was washed extensively with tap water to remove impurities such as sugars, coloring agents, and some organic and inorganic compounds, which are soluble impurities attached to the biosorbent surface until the washing water appeared clear and thoroughly rinsed with double distilled deionized water until constant pH. The rinsed residue was then filtered by Whatman Filter Paper No.41 and allowed to dry, kept in the shade of sunlight for three consecutive days. The residue was then kept in an air oven at 80 °C for 24 h; until constant weight was obtained. The effect of chemical pretreatment on the adsorption performance of LBR was investigated according to the method described by Kebede and coworkers [40].

The dried LBR was divided into three portions. The first portion of 5 g was left untreated, and then two more portions of the same amount were also transferred into 250 mL conical flasks each. The second portion was treated with 50 mL of 0.10 M HNO_3, while the third portion was treated with 50 mL of 0.10 M NaOH solution. Then, both flasks were heated at 50 °C for 4 h. The mixtures were left overnight and filtered to remove the adsorbents. Subsequently, the acid and base-treated LBR was washed repeatedly with distilled water and rinsed with double distilled deionized water until a constant pH of 7.0±0.2. The

contents of the LBR adsorbents were then similarly dried to a constant weight and converted into fine powders using an electric grinder. The grounded residues were sieved through a 1.5 mm size mesh and only the separated particles that passed through 1.5 mm were used as adsorbent material in this study [23-25]. The resulting particles were stored after drying again in the oven at 80 °C for 180 min. Finally, the sorbent residues were labeled and kept in three separate screw-capped polypropylene bottles and stored in a desiccator until use for the intended purpose. The dried but untreated LBR adsorbent material and chemically treated material were used as biosorbent.

2.4. Metal solution preparation

The stock solutions of each metal ion containing 1000 mg/L of Cd(II), Cu(II), Pb(II), and Zn(II) were prepared from their corresponding salts: $Cd(NO_3)_2 \cdot 4H_2O$, $Cu(NO_3)_2$, $Pb(NO_3)_2$, and $Zn(NO_3)_2$, respectively, by dissolving appropriate amounts of each salt in 1000 mL of distilled deionized water and filling to the mark with deionized water [41]. The resulting solutions were further serially diluted with distilled deionized water to the desired concentrations; as test solutions. The required concentration of the working solutions was prepared daily from the stock solutions and stored in the refrigerator at 4 °C. Calibration curves were plotted using the absorbance versus concentration of each metal ion throughout the experimental period.

2.5. Metal ion uptake by LBR and FAAS determination

Each metal ion interacted with a total of three residues used as adsorbents, *i.e.* two chemically modified LBR and one unmodified LBR, used as low-cost novel biosorbent materials. This was achieved by first transferring 2 g residues into three 250 mL separate conical flasks and allowed to get wet in 100 mL of double distilled deionized water. The concentrations of metal ions before and after adsorption were determined by measuring the absorbance of each metal ion using FAAS. The following analytical wavelengths were used for the determination of each metal ion studied: Cadmium 228.8 nm, copper 327.4 nm, lead 283.3 nm, and zinc 213.9 nm. Double-distilled deionized water was used as a standard solution to calibrate the instrument, which was checked periodically throughout the analysis of each metal ion for instrumental response.

2.6. Batch adsorption experiment

A series of experiments were carried out to optimize and evaluate the effects of different experimental conditions such as pH (at 2, 3, 4, 5, 7, and 9), adsorbent dose (0.5, 1.0, 1.5, 1.8, 2.0 and 2.5 g), initial concentrations of metal ions (5, 10, 20, 30, 50, 80, and 100 mg/L), contact time (30, 45, 60, 120, 180 and 240 min), and agitating speed (50, 75, 100, 150, and 200 rpm) in absorbance measurement using standard solutions prepared for each metal ion. The pH was manually adjusted with 0.10 M HCl and 0.10 M NaOH solutions and the pH meter was calibrated using buffer solutions of pH values; *i.e.* 4, 7, and 9 throughout the experiment. All adsorption experiments were conducted at room temperature (25 °C), except where the effect of temperature was studied. All adsorption experiments were conducted in a single metal system (SMS) throughout the study, *i.e.*, all tests were free from the effect of co-ions. The adsorption capacity of each metal ion and the adsorption efficiency (percent adsorption or removal) of each residue were determined as functions of each experimental parameter. For each experimental parameter, the adsorption capacity or amount of metal adsorbed (q_e) and the adsorption efficiency or percent removal (%R) were calculated based on the following relations (Equations 1 and 2) [32,42].

$$q_e = C_o - C_e \times \frac{V}{m} \tag{1}$$

$$\%R = \frac{C_o - C_e}{C_o} \times 100 \tag{2}$$

where V represents the volume of the solution, m is the adsorbent mass used, C_o is the initial concentration, and C_e is the adsorbate residual concentration in the solution.

2.7. Adsorption isotherms

The affinity of each metal ion to the freely available sites on each type of adsorbent was determined utilizing the adsorption isotherms. Both Freundlich and Langmuir models were used to describe the experimental results of metal ion adsorption by adsorbent material (the residue). The isotherm experiments were carried out with all parameters under optimized conditions for each heavy metal under study, except the temperature which was fixed at 25 °C. The initial concentration of each metal ion ranged from 20-200 mg/L. The experiment was carried out in a 250 mL conical flask that contained 100 mL of different initial concentrations prepared from each metal ion solution by residue (LBR). After reaching equilibrium in about 3 h, all flasks were filtered and the supernatant solutions were analyzed by FAAS.

The Langmuir model assumes monolayer coverage of the adsorbent surface and no interaction of the adsorbate in the plane of the adsorbent surface. The linear form of the Langmuir isotherm is given by Equation 3 [42].

$$\frac{1}{q_e} = \frac{1}{Q_o} + \frac{1}{b \times Q_o \times C_e} \tag{3}$$

where, q_e is the adsorbed analyte quantity (mg/g), C_e is the analyte concentration at equilibrium (mg/L), and Q_o and b represent the Langmuir constants at the maximum adsorption capacity (mg/g) and adsorption energy (mg/L), respectively.

Other characteristics including the shape of the Langmuir isotherm can be described in terms of a dimensionless quantity, defined as the separation factor, R_L. It also indicates whether the adsorption is favorable or not. The numerical values of adsorption for the target analytes can be calculated using Equation 4 given below [42,43]:

$$R_L = \frac{1}{1 + K_L \times C_o} \tag{4}$$

where K_L is the Langmuir constant (L/mg), C_o is the initial concentration of the adsorbate (mg/L).

On the other hand, the Freundlich isotherm is given by the following relation (Equation 5), which is a numerical expression that encompasses the heterogeneity of the surface and the exponential distribution of the sites and their energies [23].

$$q_e = K_F \times C_e^{1/n} \tag{5}$$

The Freundlich parameters, K_F and n, have to be determined in batch experiments using logarithmic regression of the data, and the linearized form of the above equation is expressed by Equation 6.

$$\log q_e = \log K_F + \frac{1}{n} \times \log C_e \tag{6}$$

2.8. Kinetics studies of adsorption of metals

The kinetic studies of each metal ion by LBR were conducted in separate flasks. The adsorption kinetics of each metal was determined, where the contact time was varied in the range from 60, 90, 120, 180, 240, 360, 480, to 720 min, to

estimate the rate determining step and study the appropriate kinetic model of each metal to the corresponding adsorbent. All experimental parameters, such as pH, adsorbent dose, contact time, agitation speed, and initial metal ion concentration, were kept at optimized values with a constant temperature of 25 °C. The sample solutions of each metal on the corresponding adsorbent were immediately filtered, and then the absorbance of the supernatant solutions was measured by FAAS. The equilibrium concentrations of each metal ion at a specified contact time were calculated to evaluate the absorption kinetics. To this end, the mechanism of adsorption was investigated by applying the pseudo-first and pseudo-second kinetic models.

The pseudo-first-order of solute sorption was evaluated using the linear equation of the following form (Equation 7) obtained by integrating the rate equation of the pseudo-first-order kinetics, rearranging for the boundary conditions [32]:

$$\log\ (q_e - q_t) = \log\ (q_e) - \frac{k_1}{2.303} \times t \tag{7}$$

where q_e and q_t are the amounts of metal adsorbed (mg/g) on the adsorbent at equilibrium and at time (t), respectively, and k_1 (1/min) is the rate constant for pseudo-first-order adsorption. From the linear graph of log (q_e–q_t) *versus* time 't', the slope and intercept values were determined and used to calculate the theoretical or calculated equilibrium adsorption capacity (q_e) and the pseudo-first-order rate constant (k_1) values, respectively.

For the absorption kinetics that follows the pseudo-second-order mechanism, the integrated basic rate equation for boundary conditions was rearranged to a linear relationship given in Equation 8 below [36]:

$$\frac{t}{q_t} = \frac{1}{K_2 \times q_e^2} + \frac{1}{q_e} \times t \tag{8}$$

where, q_e is the amount of metal adsorbed (mg/g) at equilibrium, q_t is the amount of metal adsorbed (mg/g) at time (t), and k_2 is the pseudo-second order sorption rate constant (g/mg.min). The slope and intercept values of the plot (t/q_t) *versus* time 't', were used to determine the pseudo-second-order theoretical or calculated equilibrium adsorption capacity (q_e) and its rate constant (k_2) values, respectively.

2.9. Thermodynamics studies on adsorption of metals

In order to investigate the effect of temperature under the sorption phenomenon, every experiment with each metal ion to LBR was carried out in a separate flask. To study this effect, all predetermined parameters, such as dosage, pH, contact time, concentration and agitation speed, were used in each optimized value for each metal and the temperature was established at 25, 40, 50, and 60 °C as described by Yasemin and Zeki [44]. After shaking for approximately 3 h, the sample solutions of each metal adsorbed by the corresponding adsorbent were immediately filtered. Thereafter, the supernatant solutions of each metal were measured by FAAS.

Thermodynamic parameters including the change in standard free energy (ΔG°), the change in enthalpy (ΔH°) and the change in entropy (ΔS°) were calculated using the following equations. The magnitude of ΔG° (kJ/mol) was calculated using Equations 9 and 10.

$$\Delta G^o = -R \times T \times \ln K_c \tag{9}$$

where K_c = C_e (ad) /C_e; and C_e (ad) = C_0 – $C_e \times C_e$ (ad) represents the equilibrium concentration of metal adsorbed on the surface of the adsorbents in mg/L and C_e is the corresponding equilibrium concentration of the metal in liquid phase in mg/L.

K_c is a dimensionless equilibrium constant. Vant' Hoff Equation 10 is a useful expression that links ΔH° and ΔS° with the equilibrium constant (K_c) as shown below in Equation 11 [40,45].

$$\Delta G^o = \Delta H^o - T\Delta S^o \tag{10}$$

$$\ln K_c = \frac{\Delta S^o}{R} - \frac{\Delta H^o}{R \times T} \tag{11}$$

where R is the equilibrium gas constant (R = 8.314 J/mol.K), T (K) represents the absolute temperature and K_c (cm³/g) is the standard thermodynamic equilibrium constant defined by C_e (ad)/C_e. By plotting the graph of ln K_c *versus* 1/T, the value of ΔH° and ΔS° is estimated from the slopes and intercept. Thermodynamic considerations of the adsorption process are necessary to conclude whether the process is spontaneous or not. Gibb's free energy change, ΔG°, is the fundamental criterion of spontaneity. Reactions occur spontaneously at a given temperature if the value of ΔG° is negative.

3. Results and discussion

3.1. Adsorbent characterization

The level of adsorption of metal ions on the active sites of LBR is primarily influenced by the nature of the functional groups responsible for effecting the required adsorption. The occurrence and position of the functional groups are determined by FT-IR spectral analysis, which was carried out in the range of 4000 to 400 cm⁻¹ (Figure 1). The FT-IR spectrum of the raw LBR compared to that of the metal-loaded LBR adsorbent was also studied in this range.

The broad band observed at 3431 cm⁻¹ revealed the presence of the OH and NH groups. The absorption band at 2921-2850 cm⁻¹ is related to the CH stretching modes of the CH_2 and CH groups. The band at 1740-1610 cm⁻¹ is the stretching vibration of COO⁻ and C-O, while the 1650-1500 cm⁻¹ band interval is the bending vibration of N-H. The absorption band at 1423-1417 cm⁻¹ is the phenolic O-H and C-O stretching of carboxylates. The bands at 1412 and 1032 cm⁻¹ are indicative of the bending of CH_3 and the stretching vibration of C-N, respectively. Absorptions around 1150-1000 cm⁻¹ are caused by vibrations of C-O-C and O-H in polysaccharides and 1000-500 cm⁻¹ band interval may be due to Si-H bend vibration and halogenated compounds (C–X) stretching vibration, where 'X' represents halogens [42,46]. The FT-IR spectra of LBR exposed to metal ions indicated that there were no significant shifts or changes in any of the characteristic absorbance bands at 3341, 2921, and 1036 cm⁻¹. However, the peaks at 1640 and 1463 cm⁻¹ evolved a band shift in all metals, which implies that these groups may be responsible for the affinity of heavy metal adsorption. The most effective mode of the adsorption process is most likely due to the adsorbent and adsorbate configuration [30]. No adsorption peaks evolved or were extinguished by the uptake of the metals, indicating that after adsorption of metals, no molecular bond of the structure formed or disappeared for each metal ion. Adsorption sites or quantity of heavy metals in such spectra are not a realistic indicator. However, the structural-specific changes in the adsorbents most likely indicate the adsorption of the metals. All these observations and explanations agree well with the published reports [15,17,22,41].

3.2. Effect of experimental parameters on the adsorption process

3.2.1. Effect of chemical treatment on the adsorption of heavy metals

Table 1. Effect of chemical treatment on LBR for Cd(II), Cu(II), Pb(II), and Zn(II); at the initial metal concentration C_o = 30 mg/L; pH = 4; dosage = 1 g for each adsorbent; agitation speed = 150 rpm; contact time = 120 min; and temperature = 25 °C for n = 3.

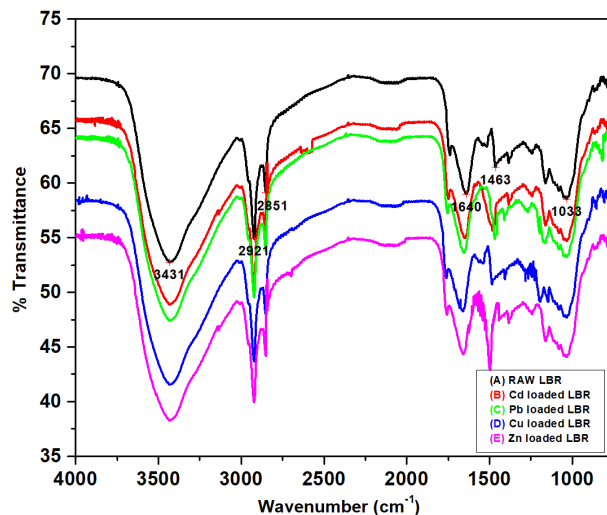| Adsorbent	Percent (%) adsorption or efficiency of adsorbents			
	Cd(II)	Cu(II)	Pb(II)	Zn(II)
Untreated LBR	92.50±0.58	90.27±2.38	95.96±1.85	81.45±2.05
0.10 M HNO₃ treated LBR	96.47±1.37	92.67±0.87	97.33±1.05	82.08±0.89
0.10 M NaOH treated LBR	95.28±0.96	92.10±1.29	98.20±0.81	81.88±1.52

Figure 1. FT-IR characterization of LBR adsorbent before (A) and after (B-E) adsorption of Cd(II) (B); Pb(II) (C); Cu(II) (D); and Zn(II) (E).

Chemical treatments are generally expected to improve biosorption capacity [35,47]. The effects of chemical treatment of the adsorbent (LBR) on the removal efficiency of each metal ion are shown in Table 1. It was observed that the removal efficiency of the chemically modified LBR adsorbent materials showed certain improvements in the adsorption performance of each adsorbent for each metal, compared to the unmodified one. This could be attributed to pretreatment of the adsorbents, which most likely results in unmasking or exposure of the metal binding sites or activation of the metal binding groups by modifying existing ones and alterations in charge density on the surface of the LBR. In this study, the LBR was modified in acidic and basic media.

3.2.2. Modification in acidic media (HNO₃)

The adsorption efficiency of the metal ions on the acid (HNO₃) modified LBR showed improved uptake than the unmodified one and even better than the base-modified LBR, except for Pb(II), as shown in Table 1. This may be due to the fact that acids can remove acid-soluble surface impurities, rupture of the cell membrane, and the resulting exposure of free binding sites or activation of functional groups presented on the adsorbent (LBR) [48]. As a result, it could probably increase the proportion of active adsorbent surfaces to be charged negatively. This could create a good environment to uptake extra metal ions than the unmodified one, and thus increase the adsorption capacity. A similar trend was also found in the literatures; for example, in the work reported by Kebede *et al.* [40], acid modification decreased the organic content of the adsorbent and resulted in increased porosity. Similarly, promising findings were also reported in which a linear relationship between the total negative charge and the amount of adsorbed copper ions was observed for twelve types of agricultural by-products after modification with citric acid [49]. In this latter work, it was learned that the total negative charges of all types of agricultural by-products increased significantly [49].

3.2.3. Modification in basic media (NaOH)

In other series of experiments, NaOH was used for the modification of LBR. The adsorption efficiencies of the metal ions (Table 1) were increased compared to the unmodified LBR. The adsorption efficiency of Pb(II) was exceptionally higher both in acid-modified and unmodified LBR. The negatively charged hydroxyl ions on the surface of the adsorbent could be the cause for the increment of adsorption efficiency compared to that of the unmodified LBR. The alkali pretreatment could also release polymers such as polysaccharides that have a high affinity for certain metal ions. The types of chemicals utilized to modify residues determine the efficiency of the LBR adsorbent to remove soluble compounds, eliminating the coloration of the aqueous solutions and thus increasing the efficiency of metal adsorption, as was also reported in the scientific literature [1,2,35,50]. Generally, three possible reasons could be stated for the increase in the adsorption capacities of metal ions, including the surface area, average pore volume, and pore diameter after alkaline treatment [40]. The adsorption capacity decreased in the order of Pb(II) > Cd(II) > Cu(II) > Zn(II) for LBR treated by NaOH. The amount of metal ions bound by the adsorption site depends on the level of modification, the nature of the metal (such as solubility) and the type of chemical substances used for modification [22].

3.2.4. Effect of pH

Metal-ion adsorption by the biosorbents may also be governed by the pH of the sample solution. The effects of pH on the removal of metal ions by LBR considered in this study are shown in Figure 2. The maximum removal of metal ions was observed at pH 5, which is 93.90% for Cd(II), 91.39% for Cu(II), 96.86% for Pb(II) and 83.95% for Zn(II). It was further noted from Figure 2 that the amount of each metal adsorbed by LBR increased rapidly at lower pH values, especially for Cd(II) and Zn(II).
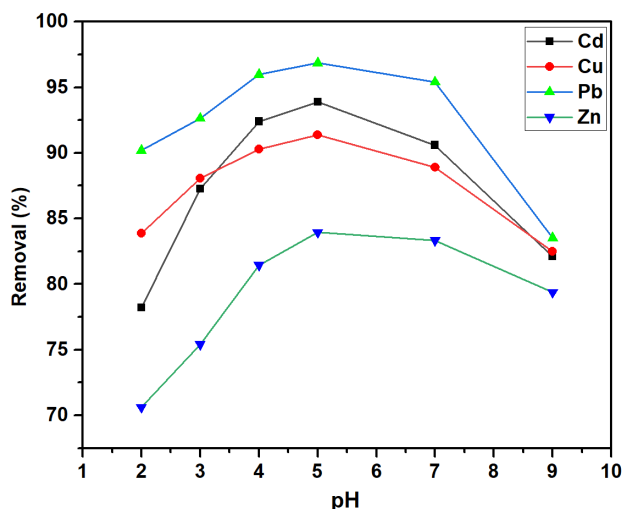
Figure 2. Effect of pH on the removal of Cd(II), Cu(II), Pb(II) and Zn(II) by LBR; at the initial concentration of metal ions C_o = 30 mg/L, dose = 1 g LBR, agitation speed = 150 rpm, contact time = 120 min and temperature at 25 °C.
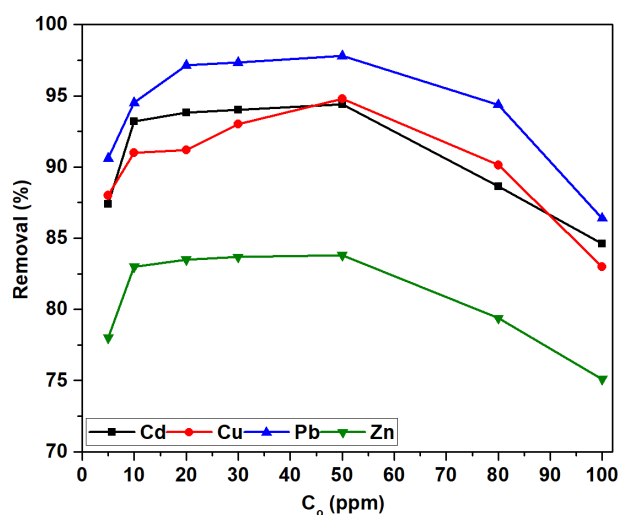

Figure 3. Effect of the initial concentrations of metal ions Cd(II), Cu(II), Pb(II), and Zn (II) on the adsorption capacity of LBR; at pH = 5 for all metals, dose = 1 g of LBR, agitation speed = 150 rpm, contact time = 120 min and temperature at 25 °C.

The experimental results obtained in this study indicated that the adsorption of Cd(II) and Zn(II) is relatively more pH dependent than Pb(II) and Zn(II). Furthermore, the adsorption capacity of each metal ion also increased with pH and then decreased when the pH increased beyond the optimum value. This could be attributed to the fact that hydrogen ions themselves are strongly competing for the active sites of LBR at lower pH values. The pH of the solution influences the specification of metal ions and the ionization of surface functional groups [47,49].

It could further be noted that binding of H⁺ ions to the adsorbents may be occurred, which could be responsible for the reduction of the metal ion adsorption [19]. However, the percentage of removal in alkaline medium, beyond pH = 7, was lowered for each metal, as shown in Figure 2. The reduced amount of metal bounded by the alkali medium may probably be due to the fact that OH⁻ ions themselves are strongly competing for the active sites of LBR. Beyond the optimum pH, the concentration of the OH⁻ ions is higher, which could be associated with the formation of hydroxy-metal ion complexes [2]. The highest percentage of removals reported for similar other adsorbents by other workers were between pH = 4 and 6;

depending on the metal and the nature of the adsorbent used [11,31]. For a similar reason, pH = 5 was selected for this study.

3.2.5. Effect of adsorbent dose

The effect of the adsorbent dose was studied and the results obtained indicated that the removal efficiency of each metal ion increased from 86.93 to 94.44% for Cd(II), 86.92 to 92.06% for Cu(II), 85.56 to 97.39% for Pb(II), and 73.33 to 85.95% for Zn(II), when the adsorbent dose of LBR increased from 0.5 to 2.5 g. After the dose of 1 g of LBR, the increase in percent adsorption was insignificant for each metal ion. This may be due to the additional active sites for metal binding with increased doses of LBR. However, there is a fast superficial adsorption onto the LBR surface, producing a lower concentration of metal solution compared to the concentration of each metal ion available at the lower dose of LBR. These results agree with other studies reported in the literature [50]. Maximum removal was found at 1 g/L of LBR dose for all metals. Thus, 1 g/L of LBR was found to be sufficient amount of LBR to maintain the equilibrium dose used for all subsequent experiments.
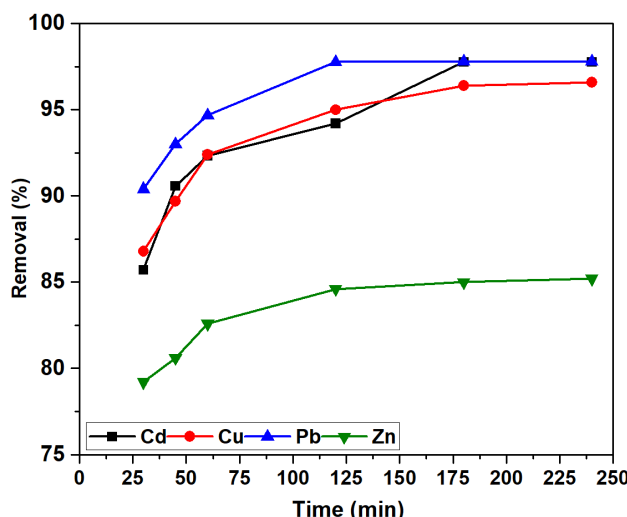
Figure 4. Effect of contact time on the removal of Cd(II), Cu(II), Pb(II), and Zn(II) by LBR; at pH = 5 for all metals, initial concentration of each metal ion at C_o = 50 mg/L, dose = 1 g of LBR, agitation speed = 150 rpm, and temperature at 25 °C.

3.2.6. Effect of initial concentration

The effect of initial concentrations of metal ions on the adsorption efficiency of LBR, carried out at different initial concentrations, ranged from 5-100 mg/L. Figure 3 showed that the removal efficiencies of LBR for all analyte metals increased rapidly as the initial metal concentration increased from 5 to 10 mg/L, and then the extent of removal was found to be gradual when the initial metal concentrations increased to 50 mg/L. However, the removal efficiency of LBR declined when the initial metal ions increased further to 100 mg/L. The percentage of metal ion removal decreases as the concentration increases, which may be attributed to the limited available sites for adsorption. However, the amount of metal ions bound in active binding sites depended on the type of metal and the concentrations of the metals studied [48,51]. Therefore, 50 mg/L was chosen as the optimum initial concentration throughout this study.

3.2.7. Effect of contact time

To establish the appropriate contact time between the LBR and the metal ion solution, the percentage removal, measured as a function of time, is given in Figure 4. For a fixed concentration of metals and mass of LBR, the percentage of removal was increased with increasing contact time for each metal. The results in Figure 4 explained that the percentage of removal of each metal was higher at the beginning. In fact, the percentage removal of all metals during the first 30 minutes was 86.80, 85.71, 90.40, and 79.20% for Cd(II), Cu(II), Pb(II) and Zn(II), respectively. The adsorption of each metal ion also showed a gradual increase for additional 20 min, and the same trend was also observed up to 180 min. This may probably be due to the saturation of the adsorbent surfaces [52]. However, the equilibrium was estimated to be attained around 180 min. Therefore, the equilibrium contact time of 180 min was selected for all further studies (Figure 4).

It is known that when the contact time increased, the adsorption capacity of each metal increased, which is proportional to the increment in percentage removal. Initially, there were a large number of active binding sites in LBR and consequently a large amount of metal ions were bound rapidly onto LBR. Therefore, the increment in percentage removal at the lower contact time might be related to the abundance of free binding sites available on LBR, which become saturated later.

The binding site was shortly become limited and the remaining vacant sites on the surface are difficult to be available for adsorption by metal ions, mainly due to the formation of repulsive forces between the metal ions on the adsorbent surface and the liquid phase [12,17,34].

3.2.8. Effect of agitation speed

It is important to determine the optimal speed that could be used in wastewater treatment. The graph of the agitation speed versus the percent adsorption for each metal is presented in Figure 5. The percentage removal of each metal increased from 92.66 to 97.74% for Cd(II), 93.46 to 96.64% for Cu(II), 94.58 to 97.87% for Pb(II) and 82.67 to 85.48% for Zn(II) when the agitation speed increased from 50 to 100 rpm and then decreased slightly with further increase of the speed to 200 rpm. Similarly, the adsorption capacity of each metal increased as the speed increased until the optimum value and then decreased when the agitation speed was increased further. This may be related to the increase in the agitation speed, the extent of mixing of the metal ions in the solution, and the increase in the active binding sites on LBR, which may be resulting in an increased percentage removal of each metal [24]. When the mixture of metal ions and LBR was shaken, the fine particles of LBR moved rapidly into the solution of each metal and this facilitates the abundance of the metal ions near the surface of the active sites. However, when the shaking speed further increased to 200 rpm and beyond, the percentage removal of each metal was slightly decreased because the high shaking speed provided sufficient additional energy to break the newly formed weak interactions/bonds between the metal ions and the binding sites of the adsorbent surface. As a result, high agitation speed may cause adsorbed metal ions to desorb from the adsorption sites [53,54]. Therefore, 100 rpm was chosen as the optimum in this study and this was in agreement with other published reports [25,34,40,46,55].

3.3. Adsorption isotherm studies

For all metal ions, the plot of straight lines obtained from C_e/q_e *versus* C_e (Equation 3) for Langmuir isotherm and log q_e *versus* log C_e (Equation 6) for Freundlich adsorption isotherm. The isotherm parameters of Langmuir and Freundlich for Cd(II), Cu(II), Pb(II), and Zn(II) adsorption, along with the corresponding correlation coefficients (R^2) are presented in

Table 2. Parameters in Langmuir and Freundlich isotherm models; for Cd(II), Cu(II), Pb(II), and Zn(II), adsorption onto LBR.

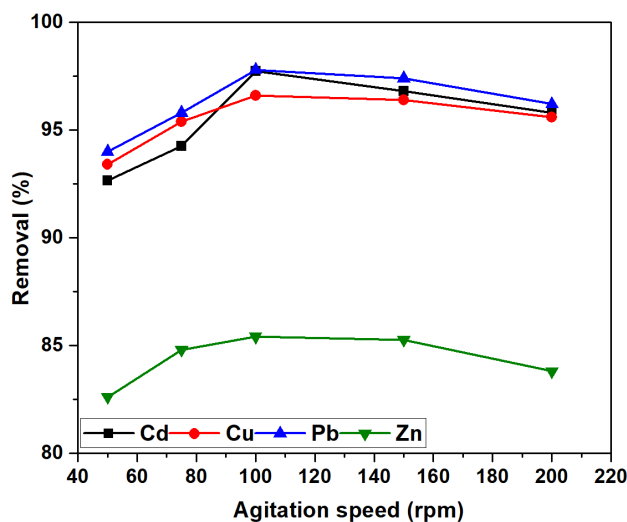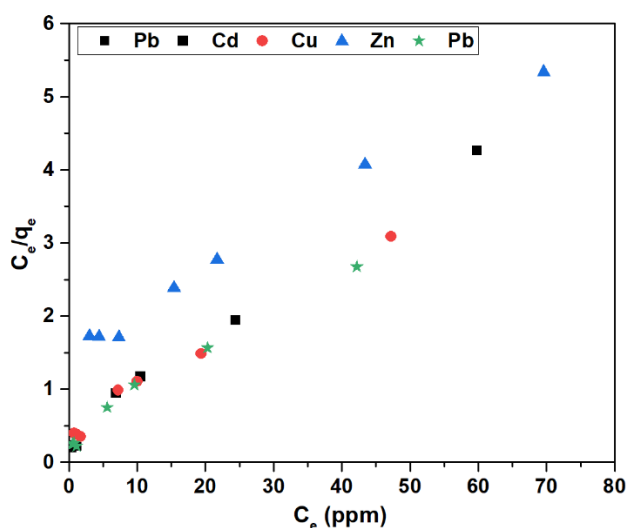| Metal ions	Adsorption isotherm models					
	Langmuir parameters			Freundlich parameters		
	Q_o (mg/g)	b (L/mg)	R^2	K_F (mg/g)	n	R^2
Cd(II)	14.925	0.238	0.991	3.508	2.660	0.945
Cu(II)	17.543	0.145	0.986	2.812	2.075	0.947
Pb(II)	16.393	0.220	0.993	3.396	2.304	0.952
Zn(II)	17.857	0.038	0.994	1.038	1.597	0.970

Figure 5. Effect of the agitation speed on the removal of Cd(II), Cu(II), Pb(II), and Zn(II) by LBR.

Figure 6. Langmuir adsorption isotherms of Cd(II), Cu(II), Pb(II), and Zn(II) by LBR.

Table 2, which indicates that the adsorption data best fitted the Langmuir adsorption isotherm for all metals studied (Figure 6) [35,49]. Therefore, homogenous surfaces mainly occur with uniform distribution of heat of adsorption over the active binding sites of LBR.

The corresponding values of adsorption capacity (K_F) in the Freundlich isotherm were 3.51, 2.81, 3.40, and 1.04 mg/g. Therefore, the Langmuir adsorption capacity (Q_o) values for each metal ion were greater than the corresponding Freundlich adsorption capacity values. Table 2 also shows that the values of Langmuir isotherm adsorption energy (b) were 0.24, 0.15, 0.22 and 0.04 for Cd(II), Cu(II), Pb(II), and Zn(II), respectively, and the corresponding Freundlich constant values related to the adsorption intensity (n), were 2.66, 2.08, 2.30, and 1.60 mg/g. The correlation coefficient (R^2) in Langmuir was

dominantly supporting the suggestion that the equilibrium data were best fitted to the Langmuir than Freundlich adsorption model [23,51].

Therefore, depending on the value of the adsorption energy (b) and the general binding energy of the active sites on LBR for each metal studied, follow the order of decreasing energy: Cd(II) > Pb(II) > Cu(II) > Zn(II), *i.e.*, at the same concentration range, Cd(II) has a higher adsorption energy or affinity in the active sites of LBR than the rest of the three metals. On the basis of the values of the adsorption intensity (n), the metals follow the same order as the binding energy, *i.e.*, Cd(II) > Pb(II) > Cu(II) > Zn(II). It is also meant that the adsorption efficiency of LBR is high enough to remove a high concentration of Cd(II) and low enough to remove a high concentration of Zn(II) at the same

Table 3. R_L values for Cd(II), Cu(II), Pb(II), and Zn(II) adsorption at different initial metal ion concentrations by LBR.

C_o (mg/L) *	R_L values of metals			
	Cd(II)	Cu(II)	Pb(II)	Zn(II)
20	0.174	0.256	0.185	0.569
30	0.123	0.186	0.131	0.469
50	0.078	0.121	0.083	0.346
80	0.051	0.079	0.054	0.248
100	0.040	0.064	0.043	0.209
150	0.027	0.044	0.029	0.150
200	0.021	0.033	0.022	0.117

* C_o: Initial metal ion concentrations.

Table 4. Pseudo-first-order and pseudo-second-order parameters; by LBR for Cd(II), Cu(II), Pb(II), and Zn(II) adsorption.

Metal ions	Kinetic models							
	Pseudo-first order				Pseudo-second- order			
	q_e (cal) [a] (mg/g)	q_e (exp) [b] (mg/g)	k_1 1/min	R^2	q_e (cal) [a] (mg/g)	q_e (exp) [b] (mg/g)	k_2 (g/g. min)	R^2
Cd(II)	0.442	4.89	0.007	0.980	4.951	4.89	0.057	0.999
Cu(II)	0.736	4.82	0.018	0.996	4.901	4.82	0.058	0.999
Pb(II)	0.058	4.89	0.031	0.943	4.926	4.89	0.106	0.999
Zn(II)	0.813	4.25	0.021	0.963	4.348	4.25	0.047	0.999

[a] q_e (cal) – calculated adsorption capacity at equilibrium time.

[b] q_e (exp) – experimental equilibrium adsorption capacity.
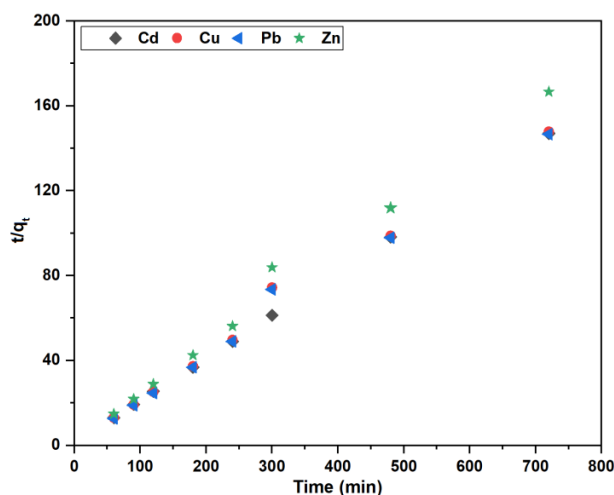
Figure 7. Pseudo-second-order kinetic models of Cd(II), Cu(II), Pb(II), and Zn(II).

concentration range of the metals applied. Thus, LBR has less efficiency to remove a high concentration of Zn(II).

The essential characteristics in the Langmuir isotherm model can be expressed in terms of a dimensionless equilibrium parameter (R_L) that is used to predict the adsorption behavior of the metals at different initial metal concentrations [1]. The adsorption data of R_L indicate a linear distribution with the initial metals' concentration ranging from 20-200 mg/L. As can be observed in Table 3, the R_L values for all metal concentrations are between 0 and 1, indicating that each metal exhibits favorable adsorption onto the active sites of LBR.

### 3.4. Kinetics of metal adsorption

The pseudo-first and pseudo-second order parameters for the adsorption of Cd(II), Cu(II), Pb(II), and Zn(II) along with the corresponding correlation coefficients (R^2) are presented in Table 4. The values of the correlation coefficients in the pseudo-second order kinetics model for each metal ion show the preferred results (R^2 = 0.999), compared to the correlations obtained for the pseudo-first order correlation values. This indicates the applicability of the pseudo-second-order kinetics model of the adsorption process between metals and biosorbent binding sites and these results agree with the literature reports for several natural adsorbents and the same initial concentration levels [31,54]. The plots of (log (q_e–q_t) *versus* time (t)) for all metal ions, both for pseudo-first-order

and pseudo-second-order kinetics were studied and established. Based on the experimental results, it was found that pseudo-second order exhibited a straight-line curve, Figure 7, while pseudo-first order resulted in an unfavorable graphical representation.

The pseudo-second-order model suggests that metal sorption is the rate-determining or controlling step in the adsorption process [19,21,45,51]. The calculated equilibrium adsorption capacity q_e (cal) from first-order and second-order equations, and the experimental equilibrium adsorption capacity, q_e (exp) (mg/g) are given in Table 4. As can be seen from Table 4, for the first-order, the calculated values for equilibrium adsorption capacity did not closely approximate the measured values of the experimental equilibrium adsorption capacity. This coupled with its lower correlation coefficient, may lead to the conclusion that the adsorption process of each metal ion was not properly described by the first-order kinetics. From the chemical reaction category (chemisorptions), the best fit for the data sets of this study is achieved by pseudo-second-order type of adsorption process [44]. On the other hand, the calculated (q_e) from the second-order kinetics model by LBR for each metal ion is very close to the experimentally determined (q_e) values. As a result, the adsorption of Cd(II), Cu(II), Pb(II), and Zn(II) on the LBR system appears to follow and is better described by a pseudo-second order kinetic model.

Table 5. Thermodynamic parameters for Cd(II), Cu(II), Pb(II), and Zn(II) adsorption at different temperatures by LBR.

Temperatures (K)	Thermodynamic parameters ΔG^o (kJ/mol)			
	Cd(II)	Cu(II)	Pb(II)	Zn(II)
298	-9.401	-8.292	-9.288	-4.416
313	-11.019	-9.046	-10.719	-5.040
323	-12.767	-9.391	-12.945	-5.506
333	-14.283	-9.820	-14.147	-5.733
R^2	0.979	0.953	0.951	0.962
ΔH^o (kJ/mol)	32.491	4.593	33.630	7.1508
ΔS^o (kJ/mol.K)	0.140	0.043	0.143	0.0389
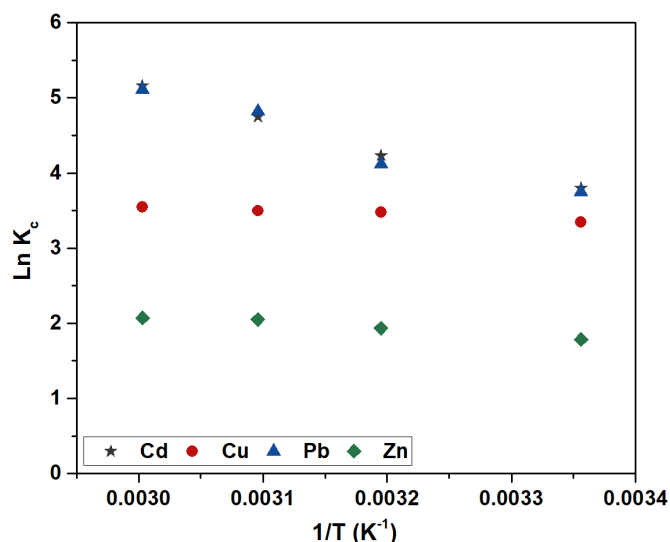
Figure 8. Thermodynamics studies of Cd(II), Cu(II), Pb(II), and Zn(II) by LBR; at pH = 5 for all metals; initial metal ions concentration = 50 mg/L; dose = 1 g of LBR.

3.5. Thermodynamics studies

The temperature of the adsorption medium could impact the energy-dependent mechanism of metal adsorption by the adsorbent. The effect of temperature on the adsorption of Cd(II), Cu(II), Pb(II) and Zn(II) ions (Figure 8) was studied at different temperatures (25, 40, 50, and 60 °C). The adsorption percentage and capacity of each metal increased with increasing temperature. This may be due to increased metal ion mobility at higher temperatures. In addition, the swelling effect within the internal structure of the adsorbent can create more active sites and enhance the adsorption capacity [56]. This effect has been observed by other researchers and may be attributed to either an increase in active sites available for adsorption on the adsorbent or a decrease in boundary layer thickness, leading to decreased mass transfer resistance and enhanced adsorption capacity [24,57].

Thermodynamic parameters (ΔG°, ΔH°, and ΔS°) that were required to determine the variables including feasibility and spontaneity of the adsorption processes, were calculated to evaluate the LBR's adsorption process with the metal ions. The plots of ln K_c *versus* 1/T for each metal ion by LBR are shown in Figure 8. Equilibrium data and thermodynamic parameters were also determined by plotting ln K_c *versus* 1/T [10]. The values of ΔH° and ΔS° could be calculated from the slopes and intercepts of the plot, respectively. All thermodynamic parameters are provided in Table 5.

The negative values of ΔG°, Table 5, indicate that the adsorption of metal ions by LBR is spontaneous and becomes more spontaneous with increasing temperature. The magnitude of ΔG° increases with temperature, indicating that the spontaneous adsorption and metal ion capacity of LBR are directly related to temperature [50]. On the other hand, positive ΔH° values of LBR indicate an endothermic adsorption process,

confirming a strong interaction between LBR and metal ions. For the metal ions to reach the adsorption sites, they must first lose their hydration shell, which requires input energy [28]. The adsorption capacity of LBR for all metals increases with temperature due to the increasing kinetic energy of the sorbent particles, which enhances adsorption through increased contact or collision frequencies between LBR and metal ions [32].

Furthermore, Table 5 shows positive ΔS° values, indicating increased entropy due to adsorption. This is caused by the redistribution of energy between the metals and the adsorbent. Before adsorption, the metal ions near the surface of the adsorbent may be more ordered than in the adsorbed state, and the ratio of free ions to those interacting with the adsorbent will be higher before adsorption. Adsorbed water molecules, which displace the metals, gain more translational energy than is lost by the metal ions, increasing the randomness in the system. As adsorption increases, the distribution of rotational and translational energy among a small number of molecules will increase, resulting in a positive ΔS° [23,44]. The effect of temperature on the mobility of metal cations was also observed to increase with adsorption [29]. The experimental results shown in Table 5 indicate that Pb(II) has the highest adsorption enthalpy, followed by Cd(II), Zn(II), and Cu(II). This may be explained by the hydration enthalpy, which reflects the ease of ion interaction with the functional groups on LBR. The more the cation is hydrated, the stronger is its hydration enthalpy and the higher its adsorption affinity [17,31,35]. The hydration enthalpies for Pb(II), Cd(II), Cu(II), and Zn(II) were 33.63, 32.49, 7.15, and 4.59 kJ/mol, respectively, signifying the high affinity of Pb(II) for the LBR surface and higher adsorption favorability compared to the other three metals [40].

4. Conclusions

In this study, a novel, low-cost, and environmentally friendly biosorbent; the local beer residue was studied for the removal of heavy metals; namely, Cd(II), Cu(II), Pb(II), and Zn(II) from contaminated water samples. The functional groups available on the surface of the raw residue (LBR) were investigated using FT-IR. The effect of chemical modification (mostly acid and base treatments) on LBR was tested. The equilibrium studies and batch adsorption parameters test (pH effect, adsorbent dose, contact time, agitation speed, and initial metal concentration), adsorption isotherms, kinetics and thermodynamics studies of the adsorbent (LBR) for each metal adsorption were investigated. Optimum values of the parameters affecting the adsorption, such as pH, adsorbent dose, contact time, agitation speed, and initial metal concentration, were obtained at 5, 1 g, 180 min, 100 rpm, and 50 mg/L, respectively.

The adsorption isotherm study of the metals on the LBR adsorbent indicated that the adsorption best fitted the Langmuir adsorption isotherm for all metals. The kinetic study of the metal adsorption also indicated that the adsorption of metals follows the pseudo-second-order model. The negative value of $\Delta G°$ and positive value of $\Delta H°$ in the thermodynamic study of the adsorption revealed that the adsorption process is spontaneous and endothermic, respectively. Sorption capacity and sorption efficiency were strongly dependent on the nature of adsorbates (metal) and adsorbent (LBR). The maximum adsorption capacity of each metal decreased in the order of Pb(II) > Cd(II) > Cu(II) > Zn(II).

The present study clearly indicated that LBR is an effective adsorbent for the removal of Cd(II), Cu(II), Pb(II), and Zn(II) from aqueous solutions with the optimized parameters. Therefore, the finding of this study suggests that the local beer residue can be used as an alternative low-cost novel adsorbent for the removal of heavy metals under study from wastewater.

Acknowledgements

Disclosure statement DS

Conflict of interest: The authors declare that they have no conflict of interest.
Ethical approval: All ethical guidelines have been adhered.
Sample availability: Samples of the compounds are available from the authors.
Data availability: All data are included in the manuscript.

CRediT authorship contribution statement CR

Conceptualization: Tesfahun Kebede; Neussie Megersa; Methodology: Tesfahun Kebede, Negussie Megersa, Henok Getachew; Software: Abi Legesse, Henok Getachew, Negussie Megersa; Validation: Negussie Megersa, Tesfahun Kebede; Formal Analysis: Henok Getachew, Negussie Megersa, Abi Legesse; Investigation: Henok Getachew, Abi Legesse; Resources: Negussie Megersa, Tesfahun Kebede; Data Curation: Abi Legesse, Henok Getachew; Writing - Original Draft: Abi Legesse, Henok Getachew; Writing - Review and Editing: Negussie Megersa, Tesfahun Kebee; Visualization: Abi Legesse, Negussie Megersa; Funding acquisition: Negussie Megersa, Tesfahun Kebede; Supervision: Neussie Megersa, Tesfahun Kebede; Project Administration: Negussie Megersa, Tesfahun Kebede.

ORCID ID and Email ✉

Tesfahun Kebede
✉ tesfakhic@gmail.com
ID https://orcid.org/0000-0002-5211-8823

Henok Getachew
✉ henokgetachew799@gmail.com
ID https://orcid.org/0009-0008-4353-3380
Abi Legesse
✉ abi.legesse@yahoo.com
ID https://orcid.org/0000-0002-3586-3477
Negussie Megersa
✉ negussie.megersa@aau.edu.et
✉ negussie.megersa@gmail.com
ID https://orcid.org/0000-0003-1255-7554

References

[1]. Sen, T. K. Agricultural solid wastes based adsorbent materials in the remediation of heavy metal ions from water and wastewater by adsorption: A review. *Molecules* **2023**, *28*, 5575.

[2]. Malik, D. S.; Jain, C. K.; Yadav, A. K. Removal of heavy metals from emerging cellulosic low-cost adsorbents: a review. *Appl. Water Sci.* **2017**, *7*, 2113–2136.

[3]. Babapoor, A.; Rafiei, O.; Mousavi, Y.; Azizi, M. M.; Paar, M.; Nuri, A. Comparison and optimization of operational parameters in removal of heavy metal ions from aqueous solutions by low-cost adsorbents. *Int. J. Chem. Eng.* **2022**, *2022*, 1–21.

[4]. Arana Juve, J.-M.; Christensen, F. M. S.; Wang, Y.; Wei, Z. Electrodialysis for metal removal and recovery: A review. *Chem. Eng. J.* **2022**, *435*, 134857.

[5]. Kyaw, H. H.; Myint, M. T. Z.; Al-Harthi, S.; Al-Abri, M. Removal of heavy metal ions by capacitive deionization: Effect of surface modification on ions adsorption. *J. Hazard. Mater.* **2020**, *385*, 121565.

[6]. United Nations World Water Assessment Programme. The United Nations World Water Development Report 2017. Wastewater: The Untapped Resource; Paris, 2017. https://www.unwater.org/ publications/un-world-water-development-report-2017 (accessed April 01, 2024).

[7]. Ondrasik, F.; Krocova, S. Toxicological aspects of wastewater. *Eur. J. Chem.* **2023**, *14*, 451–459.

[8]. Langat, F. K.; Kibet, J. K.; Okanga, F. I.; Adongo, J. O. Organic contaminants in the groundwater of the Kerio Valley water basin, Baringo County, Kenya. *Eur. J. Chem.* **2023**, *14*, 337–347.

[9]. Ali Redha, A. Removal of heavy metals from aqueous media by biosorption. *Arab J. Basic Appl. Sci.* **2020**, *27*, 183–193.

[10]. Kumar, A. Heavy metal concentrations in drinking water in the region north-east of Jhunjhunu, Rajasthan, India. *Eur. J. Chem.* **2023**, *14*, 348–352.

[11]. Pohl, A. Removal of heavy metal ions from water and wastewaters by sulfur-containing precipitation agents. *Water Air Soil Pollut.* **2020**, *231*, 503.

[12]. Saloua, J.; Mohamed, T.; Ahmed, M.; Khadija, M. Industrial rejection: Removal of heavy metals based on chemical precipitation and research for recoverable material in byproducts. *Int. J. Eng. Tech. Mgmt. Res.* **2020**, *7*, 39–52.

[13]. Zhang, Y.; Duan, X. Chemical precipitation of heavy metals from wastewater by using the synthetical magnesium hydroxy carbonate. *Water Sci. Technol.* **2020**, *81*, 1130–1136.

[14]. Hussain, S.; Ali, S. Removal of heavy metal by ion exchange using bentonite clay. *Inż. Ekol.* **2021**, *22*, 104–111.

[15]. Vidu, R.; Matei, E.; Predescu, A. M.; Alhalaili, B.; Pantilimon, C.; Tarcea, C.; Predescu, C. Removal of heavy metals from wastewaters: A challenge from current treatment methods to nanotechnology applications. *Toxics* **2020**, *8*, 101.

[16]. El Batouti, M.; Al-Harby, N. F.; Elewa, M. M. A review on promising membrane technology approaches for heavy metal removal from water and wastewater to solve water crisis. *Water (Basel)* **2021**, *13*, 3241.

[17]. Staszak, K.; Wieszczycka, K. Recovery of metals from wastewater— state-of-the-art solutions with the support of membrane technology. *Membranes (Basel)* **2023**, *13*, 114.

[18]. Covaliu-Mierlă, C. I.; Păunescu, O.; Iovu, H. Recent advances in membranes used for nanofiltration to remove heavy metals from wastewater: A review. *Membranes (Basel)* **2023**, *13*, 643.

[19]. Alghamdi, A. A.; Al-Odayni, A.-B.; Saeed, W. S.; Al-Kahtani, A.; Alharthi, F. A.; Aouak, T. Efficient adsorption of lead (II) from aqueous phase solutions using polypyrrole-based activated carbon. *Materials (Basel)* **2019**, *12*, 2020.

[20]. Jurgelane, I.; Locs, J. Activated carbon and clay pellets coated with hydroxyapatite for heavy metal removal: Characterization, adsorption, and regeneration. *Materials (Basel)* **2023**, *16*, 3605.

[21]. Sharma, G.; Sharma, S.; Kumar, A.; Lai, C. W.; Naushad, M.; Shehnaz; Iqbal, J.; Stadler, F. J. Activated carbon as superadsorbent and sustainable material for diverse applications. *Adsorp. Sci. Technol.* **2022**, *2022*, 1-21.

[22]. Wang, B.; Lan, J.; Bo, C.; Gong, B.; Ou, J. Adsorption of heavy metal onto biomass-derived activated carbon: review. *RSC Adv.* **2023**, *13*, 4275–4302.

[23]. Gebretsadik, H.; Gebrekidan, A.; Demlie, L. Removal of heavy metals from aqueous solutions using *Eucalyptus Camaldulensis*: An alternate low cost adsorbent. *Cogent Chem.* **2020**, *6*, 1720892.

[24]. Anastopoulos, I.; Robalds, A.; Tran, H. N.; Mitrogiannis, D.; Giannakoudakis, D. A.; Hosseini-Bandegharaei, A.; Dotto, G. L. Removal of heavy metals by leaves-derived biosorbents. *Environ. Chem. Lett.* **2019**, *17*, 755–766.

[25]. Baby Shaikh, R.; Saifullah, B.; Rehman, F. ur Greener method for the removal of toxic metal ions from the wastewater by application of agricultural waste as an adsorbent. *Water (Basel)* **2018**, *10* (10), 1316.

[26]. Chung, W. J.; Shim, J.; Ravindran, B. Application of wheat bran based biomaterials and nano-catalyst in textile wastewater. *J. King Saud Univ. Sci.* **2022**, *34*, 101775.

[27]. Ogata, F.; Kangawa, M.; Iwata, Y.; Ueda, A.; Tanaka, Y.; Kawasaki, N. A study on the adsorption of heavy metals by using raw wheat bran bioadsorbent in aqueous solution phase. *Chem. Pharm. Bull. (Tokyo)* **2014**, *62*, 247–253.

[28]. Altun, T.; Pehlivan, E. Removal of copper(II) ions from aqueous solutions by walnut-, hazelnut- and almond-shells. *Clean (Weinh.)* **2007**, *35*, 601–606.

[29]. Dias, M.; Pinto, J.; Henriques, B.; Figueira, P.; Fabre, E.; Tavares, D.; Vale, C.; Pereira, E. Nutshells as efficient biosorbents to remove cadmium, lead, and mercury from contaminated solutions. *Int. J. Environ. Res. Public Health* **2021**, *18*, 1580.

[30]. Okoro, H. K.; Alao, S. M.; Pandey, S.; Jimoh, I.; Basheeru, K. A.; Caliphs, Z.; Ngila, J. C. Recent potential application of rice husk as an eco-friendly adsorbent for removal of heavy metals. *Appl. Water Sci.* **2022**, *12*, 259.

[31]. Obianyo, J. I. Characterization and removal of nickel (II) from paint industry effluent by rice husk adsorbent. *Rwanda J. Eng. Sci. Technol. Environ.* **2021**, *4*(1), 1-19.

[32]. Islam, I. U.; Ahmad, M.; Ahmad, M.; Rukh, S.; Ullah, I. Kinetic studies and adsorptive removal of chromium Cr(VI) from contaminated water using green adsorbent prepared from agricultural waste, rice straw. *Eur. J. Chem.* **2022**, *13*, 78–90.

[33]. Haddad, M.; Nassar, D.; Shtaya, M. Heavy metals accumulation in soil and uptake by barley (Hordeum vulgare) irrigated with contaminated water. *Sci. Rep.* **2023**, *13*, 4121.

[34]. Medyńska-Juraszek, A.; Ćwieląg-Piasecka, I.; Jerzykiewicz, M.; Trynda, J. Wheat straw biochar as a specific sorbent of cobalt in soil. *Materials (Basel)* **2020**, *13*, 2462.

[35]. Dun, Y.; Wu, C.; Zhou, M.; Tian, X.; Wu, G. Wheat straw- and maize straw-derived biochar effects on the soil cadmium fractions and bioaccumulation in the wheat–maize rotation system. *Front. Environ. Sci.* **2022**, *10*.

[36]. Tadesse, B.; Teju, E.; Megersa, N. The *Teff* straw: a novel low-cost adsorbent for quantitative removal of Cr(VI) from contaminated aqueous samples. *Desalination Water Treat.* **2014**, 1–12, 2925-2936.

[37]. Birhanu, A. M.; Teferra, T. F.; Lema, T. B. Fermentation Dynamics of Ethiopian Traditional Beer (Tella) as Influenced by Substitution of Gesho (Rhamnus prinoides) with Moringa stenopetala: An Innovation for Nutrition. *Int. J. Food Sci.* **2021**, *2021*, 1–10.

[38]. Hotessa, N.; Robe, J. Ethiopian indigenous traditional fermented beverage: The role of the microorganisms toward nutritional and safety value of fermented beverage. *Int. J. Microbiol.* **2020**, *2020*, 11, 8891259.

[39]. Negasi, A.; Fassil, A.; Asnake, D. In vitro evaluation of lactic acid bacteria isolated from traditional fermented Shamita and Kocho for their desirable characteristics as probiotics. *Afr. J. Biotechnol.* **2017**, *16*, 594–606.

[40]. Kebede, A.; Kedir, K.; Melak, F.; Asere, T. G. Removal of Cr(VI) from aqueous solutions using biowastes: Tella residue and Pea (Pisum sativum) seed shell. *ScientificWorldJournal* **2022**, *2022*, 7554133.

[41]. Sylwan, I.; Thorin, E. Removal of heavy metals during primary treatment of municipal wastewater and possibilities of enhanced removal: A review. *Water (Basel)* **2021**, *13*, 1121.

[42]. Teju, E.; Legesse, A.; Megersa, N. The non-edible and disposable parts of oyster mushroom, as novel adsorbent for quantitative removal of atrazine and its degradation products from synthetic wastewater. *Heliyon* **2024**, *10*, e26278.

[43]. Ali, I. The quest for active carbon adsorbent substitutes: Inexpensive adsorbents for toxic metal ions removal from wastewater. *Sep. Purif. Rev.* **2010**, *39*, 95–171.

[44]. Bulut, Y.; Tez, Z. Removal of heavy metals from aqueous solution by sawdust adsorption. *J. Environ. Sci. (China)* **2007**, *19*, 160–166.

[45]. Dajan, F. T. Synthesis, characterization and study on the sorption property of Fe3O4/Al2O3/ZrO2 nanocomposites toward the removal of cadmium, lead and chromium ions from aqueous solution, MSc Thesis, Haramaya University: Haramaya, 2016. http://ir.haramaya.edu.et/hru/bitstream/handle/123456789/1262/Fekadu%20Tsegaye.pdf?isAllowed=y&sequence=1 (accessed April 01, 2024).

[46]. Nag, S.; Mondal, A.; Bar, N.; Das, S. K. Biosorption of chromium (VI) from aqueous solutions and ANN modelling. *Environ. Sci. Pollut. Res.* **2017**, *24*, 18817–18835.

[47]. Gaur, N.; Kukreja, A.; Yadav, M.; Tiwari, A. Adsorptive removal of lead and arsenic from aqueous solution using soya bean as a novel biosorbent: equilibrium isotherm and thermal stability studies. *Appl. Water Sci.* **2018**, *8*, 98.

[48]. Farhan, S. N.; Khadom, A. A. Biosorption of heavy metals from aqueous solutions by Saccharomyces Cerevisiae. *Int. J. Ind. Chem.* **2015**, *6*, 119–130.

[49]. Kiran, I.; Akar, T.; Tunali, S. Biosorption of Pb(II) and Cu(II) from aqueous solutions by pretreated biomass of Neurospora crassa. *Process Biochem.* **2005**, *40*, 3550–3558.

[50]. Osasona, I.; Adebayo, A. O.; Ajayi, O. O. Biosorption of Pb(II) from aqueous solution using cow hooves: Kinetics and thermodynamics. *ISRN Phys. Chem.* **2013**, *2013* (1), 171865.

[51]. Adane, T.; Haile, D.; Dessie, A.; Abebe, Y.; Dagne, H. Response surface methodology as a statistical tool for optimization of removal of chromium (VI) from aqueous solution by Teff (Eragrostis teff) husk activated carbon. *Appl. Water Sci.* **2020**, *10*, 1-13.

[52]. Wirtu, Y. D.; Melak, F.; Yitbarek, M.; Astatkie, H. Aluminum coated natural zeolite for water defluoridation: A mechanistic insight. *Groundw. Sustain. Dev.* **2021**, *12*, 100525.

[53]. Shen, Z.; Jin, F.; Wang, F.; McMillan, O.; Al-Tabbaa, A. Sorption of lead by Salisbury biochar produced from British broadleaf hardwood. *Bioresour. Technol.* **2015**, *193*, 553–556.

[54]. Olafadehan, O. A.; Akpo, O. Y.; Enemuo, O.; Amoo, K. O.; Abatan, O. G. Equilibrium, kinetic and thermodynamic studies of biosorption of zinc ions from industrial wastewater using derived composite biosorbents from walnut shell. *Afr. J. Environ. Sci. Tech.* **2018**, *12*, 335–356.

[55]. Mekonnen, E.; Yitbarek, M.; Soreta, T. R. Kinetic and thermodynamic studies of the adsorption of Cr(VI) onto some selected local adsorbents. *S. Afr. J. Chem.* **2015**, *68*, 45–52.

[56]. Jain, C. K. Adsorption of zinc onto bed sediments of the River Ganga: adsorption models and kinetics. *Hydrol. Sci. J.* **2001**, *46*, 419–434.

[57]. Wartelle, L. H.; Marshall, W. E. Citric acid modified agricultural by-products as copper ion adsorbents. *Adv. Environ. Res.* **2000**, *4*, 1–7.